Impulse Noise Removal Using Directional Difference Based Noise Detector and Adaptive Weighted Mean Filter

Xuming Zhang and Youlun Xiong

***Abstract*—A two-stage algorithm, called switching-based adaptive weighted mean filter, is proposed to remove salt-and-pepper noise from the corrupted images. First, the directional difference based noise detector is used to identify the noisy pixels by comparing the minimum absolute value of four mean differences between the current pixel and its neighbors in four directional windows with a predefined threshold. Then, the adaptive weighted mean filter is adopted to remove the detected impulses by replacing each noisy pixel with the weighted mean of its noise-free neighbors in the filtering window. Numerous simulations demonstrate that the proposed filter outperforms many other existing algorithms in terms of effectiveness in noise detection, image restoration and computational efficiency.**

***Index Terms*—Impulse noise, mean filter, median filter, noise detector.**

I. Introduction

IMPULSE noise removal from the degraded images is very significant for subsequent image processing operations. Among the various approaches for removing impulse noise, the median filter is used widely because of its good noise suppression ability and high computational efficiency [1]. The standard median (MED) is prone to damage such important details as thin lines and sharp corners in that it replaces every pixel by the median value of its neighboring pixels. The variations of the MED filter, such as weighted median filter [2], multistage median filter [3] and mutishell median filter [4], have been proposed to improve detail preservation ability. However, the MED filter and the above modifications are implemented invariantly for all the pixels in the image, thereby causing the alteration of the undisturbed good pixels.

An effective solution to address the above problem is to incorporate the switching-based filters, such as ranked-order based adaptive median (RAM) filter [5], progressive switching median (PSM) filter [6], adaptive center weighted median (ACWM) filter [7], Laplacian detector-based switching median (LDSM) filter [8] and pixel-wise MAD-based (PWMAD) filter [9]. In these switching-based filters, the noise detector is first adopted to realize the preliminary identification of corrupted pixels and filtering is activated for the detected impulses. Owing to the incorporation of noise detection mechanism, these filters can avoid the undue smoothing of the corrupted images. However, they perform badly in noise detection and damage the important image details or retain numerous impulses in the filtered images at a high noise ratio.

To effectively restore the highly corrupted images, some novel switching-based filters have been proposed, such as opening-closing sequence (OCS) filter [10] and switching median filter with boundary discriminative noise detection (BDND) [11]. The OCS filter adopts the mathematical residues based noise detector to identify corrupted pixels and combines the open-close sequence filter with a block smart erase method to remove the detected impulses. This filter is very effective when the noise ratio is over 40%, but it cannot preserve the image details very well at a low noise ratio due to misclassification of numerous uncorrupted pixels as noise pixels. In the BDND filter, a simple and effective BDND method is first adopted to realize impulse noise identification and then the modified noise adaptive soft-switching median (NASM) filter [12] is applied to the detected noise pixels. This filter provides higher noise detection accuracy and better filtering performance than the NASM filter, but it is time-consuming because the BDND algorithm uses a large local window with a size of 21×21 in the first iteration for impulse noise detection.

In this letter, we propose the switching-based adaptive weighted mean (SAWM) filter for salt-and-pepper noise removal. The proposed filter combines the directional difference based noise detector with the adaptive weighted mean filter to restore the corrupted images. Compared with the above switching- based filters, the proposed filter can identify salt-and-pepper noise more effectively and provide better image restoration performance and higher computational efficiency across a wide range of noise ratios.

II. Directional Difference Based Noise Detector

Let $f_{i,j}$ denote the gray-level value of the noisy image at pixel location (i,j) and $W_{i,j}$ denote the detection window of size $L_d \times L_d$ centered at (i,j), i.e., $W_{i,j} = \{(i+s, j+t) | -(L_d-1)/2 \le s,t \le (L_d-1)/2\}$. If the samples in $W_{i,j}$ are arranged by their values in increasing order, the noisy pixels will be generally located near the two ends of the increasingly ordered samples [13]. Let F_k denote the kth data item in these

Manuscript received June 04, 2008; revised November 19, 2008. Current version published February 26, 2009. This work was supported the National Natural Science Foundation of China under Grants 50835004 and 50625516. The associate editor coordinating the review of this manuscript and approving it for publication was Dr. Lap-Pui Chau.

The authors are with the School of Mechanical Science and Engineering, Huazhong University of Science and Technology, Wuhan 430074, China (e-mail: xmboshi.zhang@gmail.com; famt@hust.edu.cn).

Digital Object Identifier 10.1109/LSP.2009.2014293

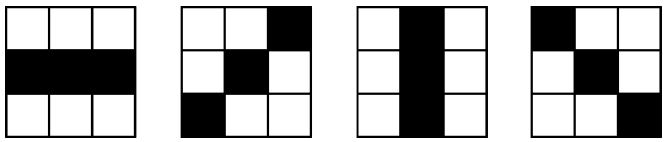

Fig. 1. Decomposition of 3 × 3 detection window.

ordered samples. The set of noise candidates in $W_{i,j}$ will be defined as

$$S_{i,j} = \{(i+s, j+t) | (i+s, j+t) \in W_{i,j} \wedge (f_{i+s,j+t} \leq F_r \vee f_{i+s,j+t} \geq F_{Z-r+1})\} \quad (1)$$

where $Z = L_d \times L_d, r$ is an integer chosen according to the type of impulse noise and $1 \leq r \leq (Z-1)/2$, "$\wedge$" and "$\vee$" are the signs of conjunction and disjunction, respectively [14].

The noise in the image has random spatial distribution while the image edge has the characteristics that image pixels along the edge direction have similar gray-level values. To fully utilize the characteristics of image edge to differentiate it from impulse noise, the detection window $W_{i,j}$ is decomposed into four subwindows as illustrated with $L_d = 3$ in Fig. 1. When $L_d \geq 5$, theoretically, more directions should be considered. But simulations show that incorporation of more directions can only provide very slightly increased noise detection accuracy at the expense of the increasing computational efficiency. So, only four directions will be considered. Four directional subwindows which exclude noise candidates are denoted as

$$W^1_{i,j} = \{(i, j+s) | (i, j+s) \in W_{i,j} \wedge (i, j+s) \notin S_{i,j}\} \quad (2)$$

$$W^2_{i,j} = \{(i+s, j-s) | (i+s, j-s) \in W_{i,j} \wedge (i+s, j-s) \notin S_{i,j}\} \quad (3)$$

$$W^3_{i,j} = \{(i+s, j) | (i+s, j) \in W_{i,j} \wedge (i+s, j) \notin S_{i,j}\} \quad (4)$$

$$W^4_{i,j} = \{(i+s, j+s) | (i+s, j+s) \in W_{i,j} \wedge (i+s, j+s) \notin S_{i,j}\}. \quad (5)$$

For any subwindow $W^k_{i,j} (1 \leq k \leq 4)$, the absolute weighted mean value of the differences between the center pixel and its neighboring pixels in this subwindow is determined as

$$\overline{d}^k_{i,j} = \begin{cases} \dfrac{\left|\sum_{(i+s,j+t) \in W^k_{i,j}} w_{i+s,j+t} d_{i+s,j+t}\right|}{\sum_{(i+s,j+t) \in W^k_{i,j}} w_{i+s,j+t},} & \text{if } W^k_{i,j} \neq \emptyset \\ F_{Z-r+1} - F_r, & \text{if } W^k_{i,j} = \emptyset \end{cases} \quad (6)$$

where $\emptyset$ denotes the null set, $d_{i+s,j+t}$ denotes the difference between $f_{i+s,j+t}$ and $f_{i,j}$, and $w_{i+s,j+t}$ is the weight of $d_{i+s,j+t}$. The weight $w_{i+s,j+t}$ is supposed to decrease with the increasing absolute value of $d_{i+s,j+t}$ to weaken the influence from large differences on the absolute weighted mean value. Through extensive simulations, we choose $w_{i+s,j+t}$ as the following decreasing function:

$$w_{i+s,j+t} = 1/(1 + |d_{i+s,j+t}|^2). \quad (7)$$

Let $D_{i,j}$ denote the minimum of four absolute weighted mean values, i.e., $D_{i,j} = \min\{\overline{d}^k_{i,j} | 1 \leq k \leq 4\}$. The minimum $D_{i,j}$ is dependant on the local features of the noisy image. If the center pixel is corrupted by impulse noise, $D_{i,j}$ will take a large value in that $f_{i+s,j+t}$ substantially differs from $f_{i,j}$ in any subwindow and the four mean values are all large. When the center pixel is a noise-free pixel located in the smooth area, $\overline{d}^k_{i,j}$ in any subwindow $W^k_{i,j}$ will be small because the pixels in $W^k_{i,j}$ have similar values and accordingly $D_{i,j}$ will take a small value. Similarly, $D_{i,j}$ will be also small if the center pixel is a noise-free edge pixel because the characteristics of the edge ensure that one of the four mean values will be small.

The above analysis shows that $D_{i,j}$ can be used as a measure for impulse noise detection. By comparing $D_{i,j}$ with a predefined threshold T, the pixel at (i, j) is classified as a noisy pixel with the binary flag $b_{i,j} = 1$ if $D_{i,j} \geq T$ or a noise-free pixel with $b_{i,j} = 0$ if $D_{i,j} < T$. The threshold T, to some degree, will influence the detection performance of the proposed noise detector. Through extensive simulations on gray-level images, we find that good detection results can be obtained for the various images using $0 < T < 10$.

III. Adaptive Weighted Mean Filter

The detected impulses will be removed by the adaptive weighted mean filter. For any detected noise pixel at (i, j), the filtering window of size $L_f \times L_f$ is used. Let $N_{i,j}$ be the number of noise-free pixels in the filtering window centered at (i, j). The filtering window size is adaptively determined according to $N_{i,j}$. Starting with $L_f = 3$, the filtering window iteratively extends outward by one pixel in its four sides until $N_{i,j} \geq 2$. The above idea of enlarging the window has been used by BDND filter, in which the window is enlarged until $N_{i,j} \geq (1/2)[L_f \times L_f]$. Our scheme has an improvement over the BDND filter by realizing the enlarging of the window until $N_{i,j} \geq 2$. Obviously, the SAWM filter can use the smaller filtering window than the BDND filter and so it has higher computational efficiency and better detail preservation ability.

Let $U_{i,j}$ denote the set of coordinates of noise-free pixels in the filtering window centered at (i, j), i.e., $U_{i,j} = \{(i+s, j+t) | b_{i+s,j+t} = 0 \wedge -(L_f - 1)/2 \leq s, t \leq (L_f - 1)/2\}$. The weighted mean of the noise-free pixels in the filtering window is determined as

$$f'_{i,j} = \frac{\sum_{(i+s,j+t) \in U_{i,j}} c_{i+s,j+t} f_{i+s,j+t}}{\sum_{(i+s,j+t) \in U_{i,j}} c_{i+s,j+t}} \quad (8)$$

where $c_{i+s,j+t}$ is the weight of $f_{i+s,j+t}$. All the weights are determined based on degree of compatibility (DOC) between two pixels. The DOC was proposed and defined by Y. Choi and R. Krishnapuram [15]. Here, the modified DOC between $f_{i+s,j+t}$ and $f_{i+m,j+n}$ is presented as (9), shown at the bottom of the next page.

From (9), it can be seen that $\mu_{i+s,j+t,i+m,j+n}$ increases with the decreasing absolute difference between $f_{i+s,j+t}$ and $f_{i+m,j+n}$. It is easy to understand that the more the number of noise-free pixels whose values are close to $f_{i+s,j+t}$, the larger $c_{i+s,j+t}$ should be to emphasize the contribution of $f_{i+s,j+t}$

to the filtering output. Thus, $c_{i+s,j+t}$ is defined as the sum of DOC between $f_{i+s,j+t}$ and its neighbors:

$$c_{i+s,j+t} = \sum_{(i+m,j+n)\in U_{i,j}} \mu_{i+s,j+t,i+m,j+n}. \tag{10}$$

The output of the switching-based adaptive weighted mean filter will be obtained by

$$g_{i,j} = b_{i,j} \cdot f'_{i,j} + (1 - b_{i,j}) \cdot f_{i,j}. \tag{11}$$

IV. Simulations

To demonstrate the effectiveness of the SAWM filter, comparisons about noise detection performance, restoration performance and computational complexity are made with the MED filter, RAM filter, PSM filter, ACWM filter, LDSM filter, PWMAD filter, OCS filter and BDND filter. The 512×512 gray-level images *Pepper*, *Lena* and *Bridge* with different features are chosen as the test images. The SAWM filter is aiming at removing salt-and-pepper type of impulse noise. Therefore, simulations are carried out for the test images corrupted by the salt-pepper impulses with noise densities varying from 10% to 80%.

The performance of the SAWM filter is mainly influenced by L_d. A bigger value for L_d can improve the overall filtering performance by achieving higher noise detection accuracy at the expense of increasing computational complexity. To achieve a trade-off between restoration performance and computational efficiency, we set $L_d = 7, r = 1, T = 2$ for the SAWM filter. For other filters, relevant parameters are tuned to achieve the best restoration results at the various noise densities.

A. Noise Detection Performance

Let N_f denote the number of noise-free pixels falsely identified as the noise ones and N_m denote the number of noise pixels misclassified as noise-free ones. Noise detection performance will be evaluated using the two parameters. Table I lists the noise detection results of the all the compared switching-based filters for image *Pepper*. From Table I, we can see that the SAWM filter provides smaller N_f values and smaller N_m values than the PSM filter, ACWM filter, LDSM filter and PWMAD filter. The RAM filter, OCS filter and BDND filter can identify the corrupted pixels accurately, but they produce larger N_f values than the SAWM filter. In particular, in the RAM filter and OCS filter, numerous uncorrupted pixels are misidentified as the noise pixels at a relatively low noise ratio. Because the SAWM filter can identify both the corrupted pixels and the uncorrupted pixels with very few or no mistakes, its noise detection performance outperforms that of other switching-based filters.

TABLE I
Noise Detection Results of the Various Filters for Image *Pepper*

Filters	N_f				N_m			
	20%	40%	60%	80%	20%	40%	60%	80%
RAM	18093	6278	1386	77	0	0	0	0
PSM	985	2673	5037	8853	2267	3725	5802	8239
ACWM	1566	2477	3146	5582	1039	1443	2149	4035
LDSM	4982	19730	28574	26562	1499	1588	1677	1727
PWMAD	1893	3522	5250	6924	1871	3033	3925	6575
OCS	20198	1779	68	8	0	0	0	0
BDND	370	370	290	127	0	0	0	12
SAWM	22	0	0	0	18	14	21	5

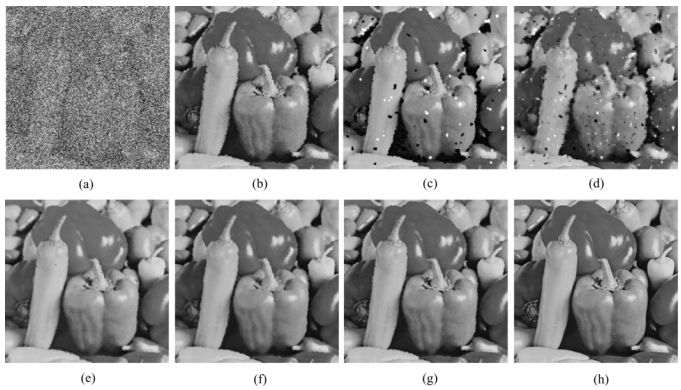

Fig. 2. Restoration results using the various filters for image Pepper corrupted by 80% impulse noise. (a) Corrupted image.(b) RAM filter. (c) PSM filter. (d) PWMAD filter. (e) OCS filter. (f) BDND filter. (g) SAWM filter. (h) Original image.

B. Restoration Performance

The restoration performance is measured by the peak signal-to-noise ratio (PSNR) defined in [10]. The PSNR values from the various filters for image *Pepper* are shown in Table II. It can be seen that the SAWM filter provides higher PSNR values than other compared filters at the various noise ratios. Fig. 2 shows that the restoration results for image *Pepper* corrupted by 80% impulse noise using the SAWM filter and five most competitive filters. Subjective visual comparisons show that the five compared filters leave noticeable impulses in the filtered images or cause the distortion of some details to a certain extent while the SAWM filter not only removes impulse noise effectively but also preserves the image details very well.

To demonstrate the generalization of the proposed filter, the performance to restore such images as *Lena* and *Bridge* is compared among these switching-based filters. The restoration results in PSNR are documented in Table III. It is easy to see

$$\mu_{i+s,j+t,i+m,j+n} = \exp\left[-\frac{|f_{i+s,j+t} - f_{i+m,j+n}|}{\frac{1}{N_{i,j}}\sqrt{\sum_{(i+p,j+q)\in U_{i,j}}(f_{i+s,j+t} - f_{i+p,j+q})^2}}\right]. \tag{9}$$

TABLE II
RESTORATION RESULTS IN PSNR (dB) OF THE VARIOUS FILTERS FOR IMAGE PEPPER

Filters	*Pepper*							
	10%	20%	30%	40%	50%	60%	70%	80%
MED	33.65	31.07	30.20	28.50	27.31	25.90	22.97	19.30
RAM	37.80	35.68	33.92	31.89	30.25	28.66	27.02	24.98
PSM	38.14	34.92	32.53	30.40	29.18	26.54	24.66	20.62
ACWM	38.35	34.17	32.35	29.52	28.25	26.56	23.31	19.37
LDSM	38.50	34.57	32.74	30.16	28.39	26.38	23.18	19.39
PWMAD	38.65	33.38	31.80	29.48	27.90	26.31	23.24	19.45
OCS	31.71	32.12	32.26	32.05	31.62	30.97	29.98	28.01
BDND	40.47	37.34	35.23	33.17	31.49	30.08	29.12	27.59
SAWM	42.78	39.37	37.32	35.35	33.84	32.33	30.86	29.07

TABLE III
RESTORATION RESULTS IN PSNR (dB) OF THE VARIOUS FILTERS FOR IMAGE LENA AND BRIDGE

Filters	*Lena*				*Bridge*			
	20%	40%	60%	80%	20%	40%	60%	80%
MED	30.39	28.17	24.67	19.45	24.62	22.53	20.74	17.20
RAM	36.28	32.20	28.85	24.98	28.62	25.85	23.32	20.39
PSM	35.99	31.38	27.40	20.88	28.14	24.56	22.21	18.23
ACWM	34.83	30.03	26.64	19.86	27.49	24.18	21.56	17.30
LDSM	34.36	29.76	26.28	19.56	27.80	24.32	21.60	17.42
PWMAD	33.49	29.39	26.34	19.71	26.86	23.75	21.28	17.36
OCS	31.30	31.20	30.55	27.95	24.32	24.31	23.81	22.07
BDND	39.09	34.28	30.17	27.63	31.54	27.86	24.90	22.34
SAWM	40.02	35.88	32.63	29.17	32.18	28.53	25.99	23.20

TABLE IV
RUNTIME OF CPU IN SECONDS OF THREE FILTERS FOR IMAGE *PEPPER*

Filters	*Pepper*							
	10%	20%	30%	40%	50%	60%	70%	80%
OCS	2.242	2.225	2.205	2.189	2.173	2.157	2.167	2.716
BDND	1.394	1.414	1.433	1.510	1.660	1.830	1.920	1.877
SAWM	0.695	0.822	0.873	0.890	0.894	0.905	0.923	0.912

that the SAWM filter also outperforms other compared filters in PSNR measurement for these images, which indicates its excellent adaptability to the various images.

C. Computational Complexity

To demonstrate the advantage of the SAWM filter in computational complexity over such most recently proposed filters as OCS filter and BDND filter, the runtimes of the three filters are compared. To make a reliable comparison, each of these filters is run 10 times on a Personal Computer equipped with 2.4-GHz CPU and 512-M RAM memory and the mean values of the runtimes are calculated for each of them. Here, it should be noted that for the BDND filter, the histogram algorithm [16] is adopted to realize the first iteration in noise detection. Table IV lists the average runtimes in seconds for these filters operating on image *Pepper*. It can be seen that the SAWM filter has less runtimes than the other filters at the various noise ratios and thus it is of lowest computational complexity among the compared filters.

V. CONCLUSION

The proposed SAWM filter is highly effective for removing impulse noise from the corrupted image. The directional difference based noise detector can realize accurate noise detection, thus facilitating the prevention of image degradation resulting from the undetected noise pixels and misidentified noise-free pixels. The adaptive weighted mean filter can remove the detected impulses effectively while preserving the details very well because it adaptively determines the filtering window size and attaches different importance to the noise-free pixels in the filtering window. The combination of the novel noise detector with the distinctive mean filter provides the SAWM filter with significantly better noise detection performance, restoration performance and computational efficiency than numerous switching-based filters.

REFERENCES

[1] A. Bovik, *Handbook of Image and Video Processing*. New York: Academic, 2000.
[2] L. Yin, R. K. Yang, M. Gabbouj, and Y. Neuvo, "Weighted median filters: A tutorial," *IEEE Trans. Circuits Syst II., Analog Digit. Signal Process.*, vol. 43, no. 3, pp. 157–192, Mar. 1996.
[3] J. Siu, J. Li, and S. Luthi, "A real time 2-D median based filter for video signals," *IEEE Trans. Consumer Electron.*, vol. 39, no. 2, pp. 115–121, May 1993.
[4] C. J. Juan, "Modified 2_D median filter for impulse noise suppressing in a real time system," *IEEE Trans. Consumer Electron.*, vol. 41, no. 1, pp. 71–81, Feb. 1995.
[5] H. Hwang and R. A. Haddad, "Adaptive median filters: New algorithms and results," *IEEE Trans. Image Process.*, vol. 4, no. 4, pp. 499–502, Apr. 1995.
[6] Z. Wang and D. Zhang, "Progressive switching median filter for the removal of impulse noise from highly corrupted images," *IEEE Trans. Circuits Syst. II., Analog Digit. Signal Process.*, vol. 46, no. 1, pp. 78–80, Jan. 1999.
[7] T. Chen and H. R. Wu, "Adaptive impulse detection using center-weighted median filters," *IEEE Signal Process. Lett.*, vol. 8, no. 1, pp. 1–3, Jan. 2001.
[8] S. Zhang and M. A. Karim, "A new impulse detector for switching median filters," *IEEE Signal Process. Lett.*, vol. 9, no. 11, pp. 360–363, Nov. 2002.
[9] V. Crnojevic, V. Senk, and Z. Trpovski, "Advanced impulse detection based on pixel-wise MAD," *IEEE Signal Process. Lett.*, vol. 11, no. 7, pp. 589–592, Jul. 2004.
[10] Z. Deng, Z. Yin, and Y. Xiong, "High probability impulse noise-removing algorithm based on mathematical morphology," *IEEE Signal Process. Lett.*, vol. 14, no. 1, pp. 31–34, Jan. 2007.
[11] P.-E. Ng and K.-K. Ma, "A switching median filter with boundary discriminative noise detection for extremely corrupted images," *IEEE Trans. Image Process.*, vol. 15, no. 6, pp. 1506–1516, Jun. 2006.
[12] H. L. Eng and K. K. Ma, "Noise adaptive soft-switching median filter," *IEEE Trans. Image Process.*, vol. 10, no. 2, pp. 242–251, Feb. 2001.
[13] R. C. Gonzalez and R. E. Woods, *Digital Image Processing*. Englewood Cliffs, NJ: Prentice-Hall, 2001.
[14] I. Aizenberg and C. Butakoff, "Effective impulse detector based on rank-order criteria," *IEEE Signal Process. Lett.*, vol. 11, no. 3, pp. 363–366, Mar. 2004.
[15] Y. Choi and R. Krishnapuram, "A robust approach to fuzzy enhancement based on fuzzy logic," *IEEE Trans. Image Process.*, vol. 6, no. 6, pp. 808–825, Jun. 1997.
[16] T. S. Huang, G. J. Yang, and G. Y. Tang, "Fast two-dimensional median filtering algorithm," *IEEE Trans. Acoust., Speech, Signal Process.*, vol. ASSP-1, no. 1, pp. 13–18, Jan. 1979.